Atmos. Chem. Phys., 12, 9881–9892, 2012
www.atmos-chem-phys.net/12/9881/2012/
doi:10.5194/acp-12-9881-2012

Atmospheric Chemistry and Physics

Aircraft measurements of wave clouds

Z. Cui[1], **A. M. Blyth**[1,2], **K. N. Bower**[3], **J. Crosier**[2,3], **and T. Choularton**[3]

[1]Institute for Climate and Atmospheric Science, School of Earth and Environment, University of Leeds, UK
[2]National Centre for Atmospheric Science, UK
[3]Centre for Atmospheric Science, SEAES, University of Manchester, UK

Correspondence to: Z. Cui (z.cui@leeds.ac.uk)

Received: 6 March 2012 – Published in Atmos. Chem. Phys. Discuss.: 29 May 2012
Revised: 25 September 2012 – Accepted: 10 October 2012 – Published: 29 October 2012

Abstract. In this paper, aircraft measurements are presented of liquid phase (ice-free) wave clouds made at temperatures greater than −5 °C that formed over Scotland, UK. The horizontal variations of the vertical velocity across wave clouds display a distinct pattern. The maximum updraughts occur at the upshear flanks of the clouds and the strong downdraughts at the downshear flanks. The cloud droplet concentrations were a couple of hundreds per cubic centimetres, and the drops generally had a mean diameter between 15–45 µm. A small proportion of the drops were drizzle. The measurements presented here and in previous recent studies suggest a different interaction of dynamics and microphysics in wave clouds from the accepted model. The results in this paper provide a case for future numerical simulation of wave cloud and the interaction between wave and cloud.

1 Introduction

Wave clouds are produced when air passes over obstacles such as mountains or islands in specific environmental conditions. The classical problem of small amplitude, two-dimensional mountain waves can be analyzed with the Scorer parameter (Scorer, 1949)

$$l^2 = \left(\frac{N}{U}\right)^2 - \frac{1}{U}\left(\frac{d^2U}{\mathrm{d}z^2}\right)^2, \quad (1)$$

where N is the Brunt Väisälä frequency, U is the mean wind speed of the flow normal to the mountain, and z is the height above ground. The Scorer parameter is used to distinguish flow regimes. In the regime of large Scorer parameter (i.e., the Scorer parameter > wavelength), buoyancy force plays a more important role than horizontal advection. The time an air parcel takes to pass over the orography is greater than it takes for vertical oscillation due to atmospheric stratification. In this case, mountain waves can be supported. Although the linear theories have provided a concise and clear picture of mountain waves (e.g. Wood, 2000), they cannot describe large-amplitude waves which are related to wave clouds. In addition, moist processes are not considered in simple theoretical studies. Cotton et al. (2010) and Lin (2007) describe the problems of classical mountain waves, such as nonlinear waves, the effect of moist processes, and three-dimensionality of terrains. A number of unique wave cloud types are observed over and near mountains: cap clouds, banner clouds, lenticular clouds and lee waves clouds (Ludlam, 1980). Wave clouds attract research in cloud microphysics for three reasons. First, the thermodynamic and kinematic conditions of wave clouds are relatively steady during their life times. Second, the ranges of temperature, humidity, and vertical velocity of wave clouds are similar to laboratory-like settings, especially for ice formation and development (e.g. Baker and Lawson, 2006). Finally, the laboratory-like nature of wave clouds make them useful for instrument validation. For those reasons, previous wave cloud studies have focused on the ice nuclei and ice particles, particularly lenticular clouds because of the stationary feature with respect to the mountain (e.g. Cooper and Saunders, 1980; Cooper and Vali, 1981; Politovich and Vali, 1983; Twohy et al., 1997; Baumgardner and Gandrud, 1998; Jensen et al., 1998; Field et al., 2001, 2012; Baker and Lawson, 2006; Heymsfield et al., 2011).

Moist processes can influence flow induced by mountain waves because condensational heating and evaporative cooling can alter atmospheric stratification (Cotton et al., 2010).

The inclusion of moist processes generally weakens the amplitude of mountain waves (Durran and Klemp, 1982). Moreover, the interaction between mountain waves and clouds can influence the organization of clouds (Clark et al., 1986; Kuettner et al., 1987).

Gravity waves play an important role in cloud organisation (e.g. Clark et al., 1986; Clark and Hauf, 1986; Kuettner et al., 1987). Clark et al. (1986) and Clark and Hauf (1986) found that boundary layer eddies and cumulus clouds can excite gravity waves that propagate horizontally and vertically. The boundary layer eddies perturb the capping inversion and induce gravity waves. Cumulus clouds act as obstacles in the flow with wind shear, develop positive pressure perturbations on the upshear flanks and negative pressure perturbations on the downshear flank, and excite gravity waves. The excited gravity waves can feedback on the boundary layer eddies, causing a change in the spacing of cloud lines.

A mountain-wave cloud is defined as "a cloud that forms in the rising branches of mountain waves and occupies the crests of the waves" (Glickman, 2000). However, in a study of the effect of moisture on mountain waves, Durran and Klemp (1982) showed that cloudy regions occurred in the wave crests (i.e., between strongest updraught and strongest downdraught) with unperturbed relative humidity RH = 90 % prior to being perturbed by the waves. The upward (downward) motion induced by the waves will increase (decrease) the real humidity such that in the wave crests the relative humidity reaches supersaturation allowing clouds to form. Clark et al. (1986) found that gravity waves play an important role in the vertical velocity of air surrounding the cloud. Their simulated clouds have clear air updraughts occurring both in front and overhead on the upshear side and clear downdraughts both in the rear and overhead on the downshear side. They found the persistence of the cloud root updraught in all cases in their simulations, i.e., the persistence of updraught below cloud base. The cloud roots are rather transient in structure and amplitudes in spite of the fact that the boundary layer eddies are quite persistent. They found that the waves and the eddies below cloud bases are more or less coupled to each other in the vertical but do propagate through the cloud field.

Heymsfield and Miloshevich (1995) studied the influence of relative humidity and temperature on wave cloud formation and evolution using aircraft measurements. They showed that cloud occurred between the maximum updraught and maximum downdraught. The relative humidity, which was governed by homogeneous ice nucleation, attained its maximum in the middle of the cloud where the temperature was lowest.

Mountain waves and mountain wave clouds have been observed over the British Isles using very high frequency radar (Worthington, 1999), gliders (Stromberg et al., 1989), aircraft measurements (Brown, 1983), radiosondes (Shutts and Broad, 1993), and satellite (Vosper and Parker, 2002). The observational studies have revealed the statistics of mountain wave clouds and the vertical momentum flux which is important for parameterizing gravity wave drag in numerical models. With the advances in aircraft measurements, it is possible to measure the horizontal structure of mountain wave clouds in terms of thermodynamics and microphysics such as in the T-Tex project (Grubišić et al., 2008). The Aerosol Properties, PRocesses And Influences on the Earth's climate (APPRAISE) programme is a Natural Environment Research Council (NERC) funded UK programme aimed at investigating the science of aerosols and their effects on climate. During the APPRAISE-clouds project, aircraft flights were undertaken to measure the cloud dynamical and microphysical properties of a range of cloud types, mainly during the winter-time over the UK (e.g. Crosier et al., 2011; Westbrook and Illingworth, 2011; Crawford et al., 2012). The UK BAe 146 Facility for Airborne Atmospheric Measurement (FAAM) aircraft, fitted with a range of state-of-the-art instruments was used to make these observations. On 27 February 2009 (flight designation B432) the aircraft flew through wave clouds over Scotland at several levels ($T > -5\,^{\circ}\mathrm{C}$) and measured meteorological parameters (e.g. temperature, wind speeds) and cloud properties. There have been no previous reports of wave cloud observations at such high temperatures with detailed in-situ flight measurements. This paper will present the structure of wave clouds. The results of the study will provide an opportunity for numerical study of the impact of moist processes on mountain waves and wave-cloud interaction with models.

2 Instrumentation and flight track

2.1 Instruments

The BAe 146 aircraft was equipped with instruments to measure aerosols, microphysics of clouds, dynamics and state parameters of air. The Nevzorov LWC-TWC probe is a constant-temperature, hot-wire probe that measures the cloud liquid and total water content. The ice water content can thus be derived. The measurement accuracy of the Nevzorov probe is given as ±10–15 % (Korolev et al., 1998). The Johnson-Williams liquid content probe measures liquid water content in clouds using a heated wire resistance bridge at a frequency of 4 Hz. Its operating range is 0–3 $\mathrm{g\,m^{-3}}$ and the typical overall uncertainty under normal operation is estimated at ±10 % (Strapp and Schemenauer, 1982). The true air temperature was measured using Rosemount de-iced and non de-iced platinum-resistance immersion thermometers. Overall, for a typical clear air measurement it is estimated to be accurate to $\pm 0.3\,^{\circ}\mathrm{C}$, but there are additional errors due to sensor wetting or the application of deicing heat (Lawson and Cooper, 1990; Friehe and Khelif, 1992). The dew-point temperature is measured with the General Eastern GE 1011B Chilled Mirror Hygrometer. A typical limitation of a chilled mirror instrument is that it is often difficult to distinguish the

phase of the condensate layer when the temperature is below 0 °C.

The Stratton Park Engineering Company (SPEC) 2D-S-128 shadow imaging probe uses a 128 photodiode linear array to detect 2-D cloud particles passing through the sample volume. The 2D-S counts and images particles up to 1.3 mm, with a response time about 10 times faster than that of the older 2D-C (cloud) probe. Its greatly improved determination of sample volume and sizing of particles of ($50\,\mu m \leq d \leq 100\,\mu m$) diameter (Lawson et al., 2006) provides significantly improved measurements of particles in this important size range. The SPEC Cloud Particle Imaging (CPI) instrument (Lawson et al., 2001) images cloud particles with diameter $d \approx 10\,\mu m$ and larger, although at small sizes ($d < 50\,\mu m$) it becomes difficult to use the CPI to distinguish the ice crystal habit of small particles ($d < 50\,\mu m$) unambiguously due to having insufficient pixels to determine their shape (Connolly et al., 2007). The Droplet Measurement Technologies (DMT) Cloud Droplet Probe (CDP) is a single-particle instrument that measures the light scattered from a droplet passing through an open path laser beam. The CDP uses a diode laser, with a single mode elliptical Gaussian beam roughly 2 mm × 0.2 mm, to count and size individual water droplets in the diameter range of 3–50 µm (Lance et al., 2010). There were no anti-shattering (Korolev) type tips on any of these probes for this flight.

The performance of Nevzorov and CDP probes have been examined (e.g. Korolev et al., 1998, Isaac et al., 2006; Schwarzenboeck et al., 2009; Lance et al., 2010). Korolev et al. (1998) found that the integrated collection efficiency of the Novzorov probe for the sensor of LWC varied between 0.9 and 1 without drops larger than 100 µm in diameter, but the efficiency for drops smaller than 5 µm could be as low as 0.6. Schwarzenboeck et al. (2009) further studied the response of the Nevzorov hot wire probe and found that droplets smaller than 20–30 µm partly tend to curve around the LWC sensor. Isaac et al. (2006) pointed out that the Nevzorov total water probe and other similar hot-wire sensors provided underestimates possibly liquid water content in the presence of large drops. Korolev et al. (1998) estimated an absolute accuracy of the Nevzorov LWC probe as 10–15 % for liquid droplets in the size interval 10–50 µm. Lance et al. (2010) used the glass bead and polystyrene latex spheres for calibration. They found that the CDP oversized droplets smaller than 20 µm and a better agreement was achieved with a 2 µm offset.

2.2 Atmospheric conditions and flight pattern

There was a ridge of high pressure over the UK on 27 February 2009 and the flow was westerly over Scotland. Wave clouds were observed in satellite images over Northern Ireland and Scotland on 27 February 2009 (Fig. 1). The vertical profiles of potential temperature and wind speed obtained using the BAe 146 are shown in Fig. 2. The data are presented

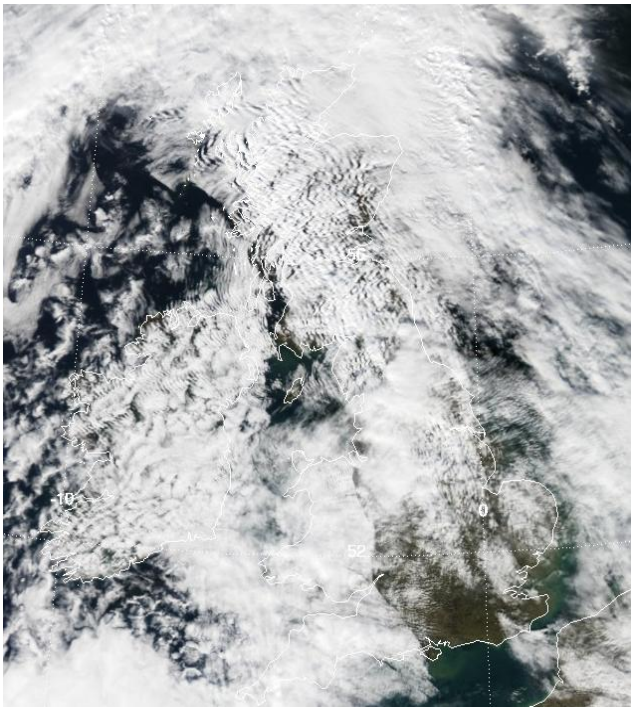

Fig. 1. The MODIS visible satellite image for the UK at 13:05 UTC on 27 February 2009.

in Table 1. There was an inversion layer at $z \approx 1.8$ km. The layer between $z = 1.6$ km and $z = 1.8$ km was close to neutral stability, and winds were variable. The wind speed increased with height within the inversion layer and gradually for about another 400 m above the layer. There were maxima at $z \approx 2250$ m in u and v components (of about 15 and 8 m s^{-1}, respectively). The measurements of the wave clouds took place between the region southwest of the Grampian Mountains and the Central Lowlands. The topography in the measurement region is varied including mountains or hills, and lochs. The highest mountains was above 1000 m and these features perturbed the south-westerly flow and excited mountain waves in the stable layer. These conditions favour the formation of cloud bands over the UK (Weston, 1980).

The aircraft flew in the wave clouds over Scotland at several levels. The first run was towards the east at $z \approx 1.65$ km above sea level (a.s.l.). Subsequent runs were carried out after a turn and a short profile ascent (see Fig. 3). The aircraft penetrated the wave clouds during Runs 1–4. In Runs 5 and 6, the aircraft encountered small lenticular capping clouds formed above the crest of the wave clouds below. Run 7, at $z \approx 2.6$ km, was in clear air above the clouds. The temperature range in Runs 1–6 was between 4.4 and −4.4 °C.

Table 1. Profiles of pressure (hPa), height (m), temperature (K), dew-point temperature T_d (K), u and v ($m\,s^{-1}$).

Pressure	Altitude	T	T_d	u	v
746.55	2502.9	273.09	257.13	14.91	5.28
751.30	2452.3	272.96	258.90	14.47	5.14
755.47	2408.1	273.09	262.92	14.80	6.04
760.17	2358.7	273.35	266.90	14.75	6.51
765.29	2305.0	273.34	270.84	15.27	7.90
770.21	2253.8	273.99	269.74	15.93	8.45
774.50	2209.3	274.11	262.06	15.64	8.42
779.74	2155.3	274.15	255.16	15.02	8.50
784.53	2106.1	274.36	250.26	14.22	8.25
789.43	2056.0	274.66	246.40	13.84	8.12
794.24	2007.1	274.80	245.91	13.49	7.74
799.83	1950.6	275.18	242.31	13.18	7.83
800.49	1943.9	275.16	241.98	13.19	7.89
801.17	1937.1	275.13	241.66	13.21	8.02
801.85	1930.2	275.15	241.33	13.08	7.98
802.56	1923.1	275.18	241.02	12.81	7.81
803.25	1916.2	275.20	240.72	12.72	7.77
804.63	1902.4	275.16	240.15	12.41	7.82
805.28	1895.8	275.24	239.88	12.23	7.53
807.22	1876.4	275.15	239.18	11.86	7.39
807.89	1869.7	275.23	238.99	11.74	7.26
809.81	1850.5	274.63	239.08	9.66	5.83
810.45	1844.1	274.62	240.27	9.70	5.68
811.85	1830.2	274.89	242.33	9.26	5.26
812.53	1823.4	274.59	243.32	8.16	4.65
813.29	1815.9	274.11	244.29	7.06	4.35
813.94	1809.4	273.98	245.24	6.80	4.33
814.56	1803.2	273.94	246.16	6.58	4.54
815.37	1795.1	273.16	247.07	5.95	4.42
816.20	1786.9	272.90	247.96	5.26	3.65
816.78	1781.2	272.06	248.84	5.36	4.35
818.12	1767.9	271.70	250.55	4.97	4.89
818.76	1761.6	271.65	251.38	4.98	4.44
819.59	1753.4	271.56	252.19	4.58	4.05
820.81	1741.3	271.46	253.78	4.65	3.65
821.29	1736.5	271.55	254.55	3.99	4.19
822.51	1724.5	271.65	256.05	4.68	4.38
824.37	1706.2	271.54	258.19	4.89	3.96
825.14	1698.7	271.58	258.87	4.37	2.94
825.72	1692.9	271.54	259.55	4.55	2.49
826.71	1683.2	271.62	260.86	4.87	3.87
827.41	1676.4	271.64	261.50	5.32	3.21
828.04	1670.1	271.77	262.13	4.65	3.80
828.46	1666.1	271.80	262.75	4.86	3.78
828.89	1661.9	271.86	263.35	5.41	4.95
830.30	1648.0	271.97	264.54	4.55	3.99
830.67	1644.4	271.93	265.11	4.58	3.40
830.98	1641.4	271.95	265.68	4.51	3.56
831.38	1637.4	272.05	266.24	4.27	4.19
832.13	1630.2	272.05	266.78	4.10	3.79
832.60	1625.6	272.11	267.85	4.27	4.40
833.21	1619.7	272.14	268.37	3.92	4.46
834.03	1611.6	272.29	270.35	4.06	3.98

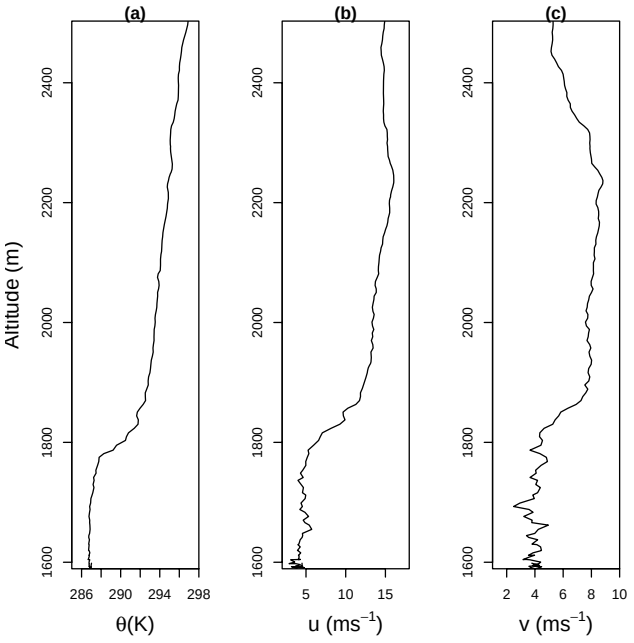

Fig. 2. Profiles of potential temperature **(a)**, horizontal wind speeds **(b, c)** sampled by the BAe 146.

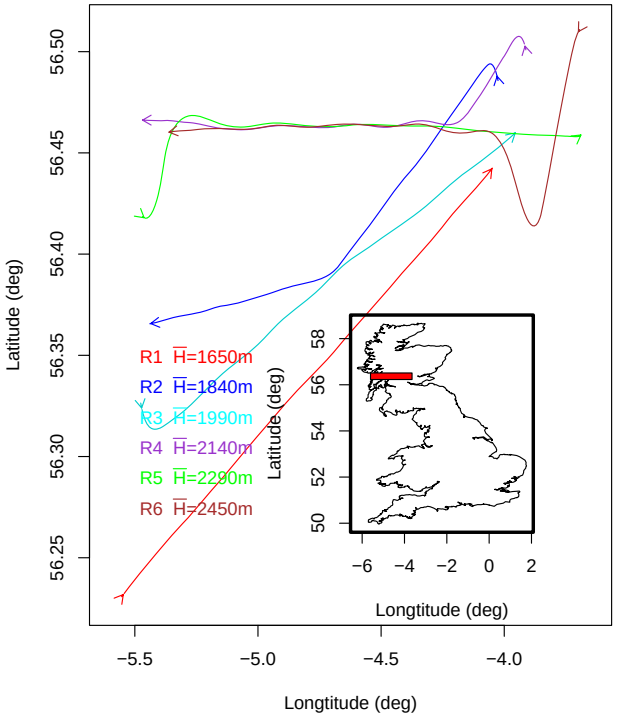

Fig. 3. Flight track of Runs 1–6 and the mean altitude of each run. The red box in the inset shows the location of the figure. Please note the figure is not in proportion in terms of distance in latitudinal and longitudinal directions.

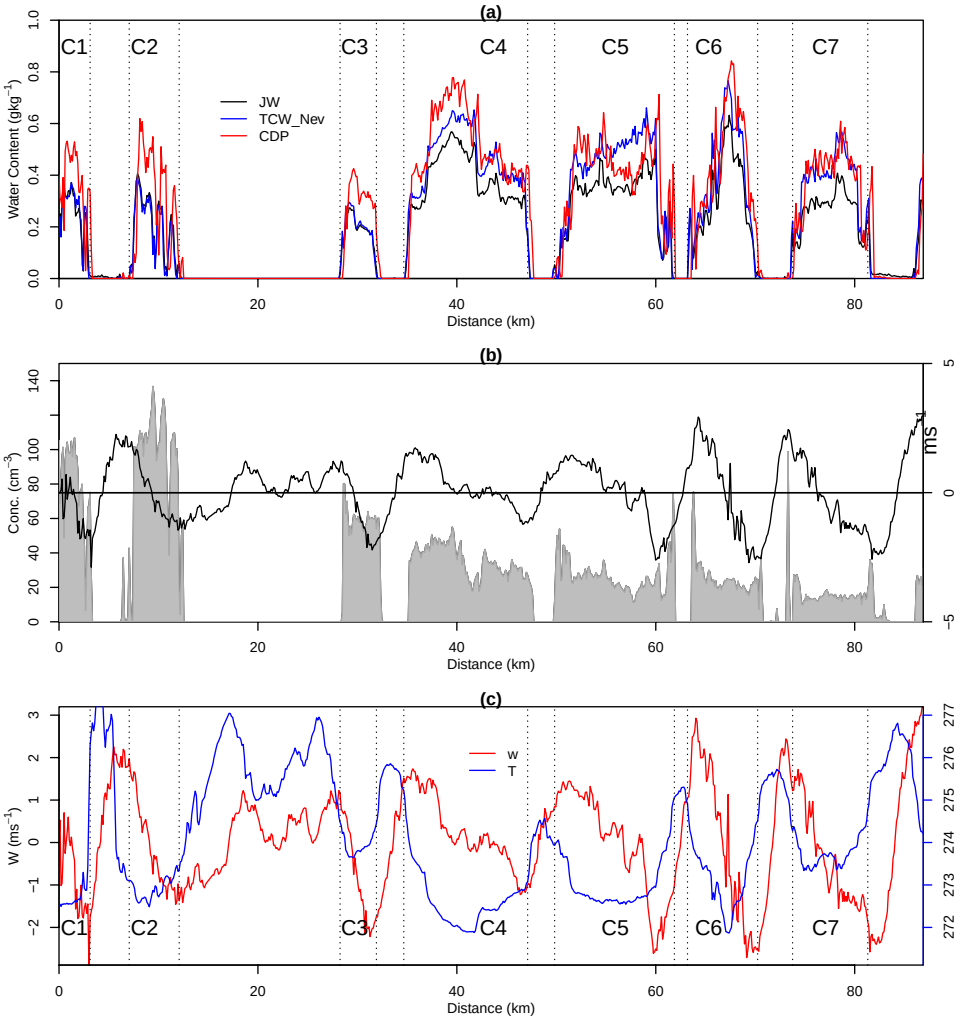

Fig. 4. (a) The LWC measured by the Johnson-Williams probe, the Nevzorov total cloud water, and as derived from the CDP, **(b)**, concentration with CDP in grey shade and vertical velocity in black curve **(b)**, and vertical velocity in red and temperature in blue **(c)** in Run 1.

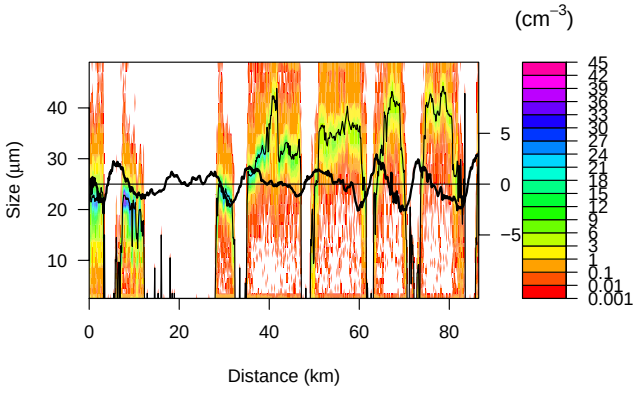

Fig. 5. Size distribution function (filled contour) obtained from CDP data for Run 1, vertical velocity (thick black curve) and the mean volume diameter (thin black curve).

3 Structure of wave clouds

The first run was at $z \approx 1.65$ km ASL towards the east. Three clouds were penetrated and these are labelled C1, C2 and C3 in Fig. 4. After C3, the aircraft gently climbed 200 feet because of the rising terrain and continued penetrating clouds C4, C5, C6 and C7. The liquid water contents from three different onstruments are shown in Fig. 4a. The maximum values encountered in the clouds were between 0.3 and 0.8 g kg^{-1}. The maximum concentrations of cloud particles measured with the CDP were around 100 cm^{-3} (Fig. 4b). The horizontal wind was from the south-west at this level. The vertical velocity, w, displays a distinct pattern with respect to the location of clouds. The maximum value of w was on the upshear sides of the clouds and the minimum on the downshear sides. The maxima were often measured outside of the clouds. It is clearly seen that the variations of both the vertical velocity and temperature (T) are wave-like

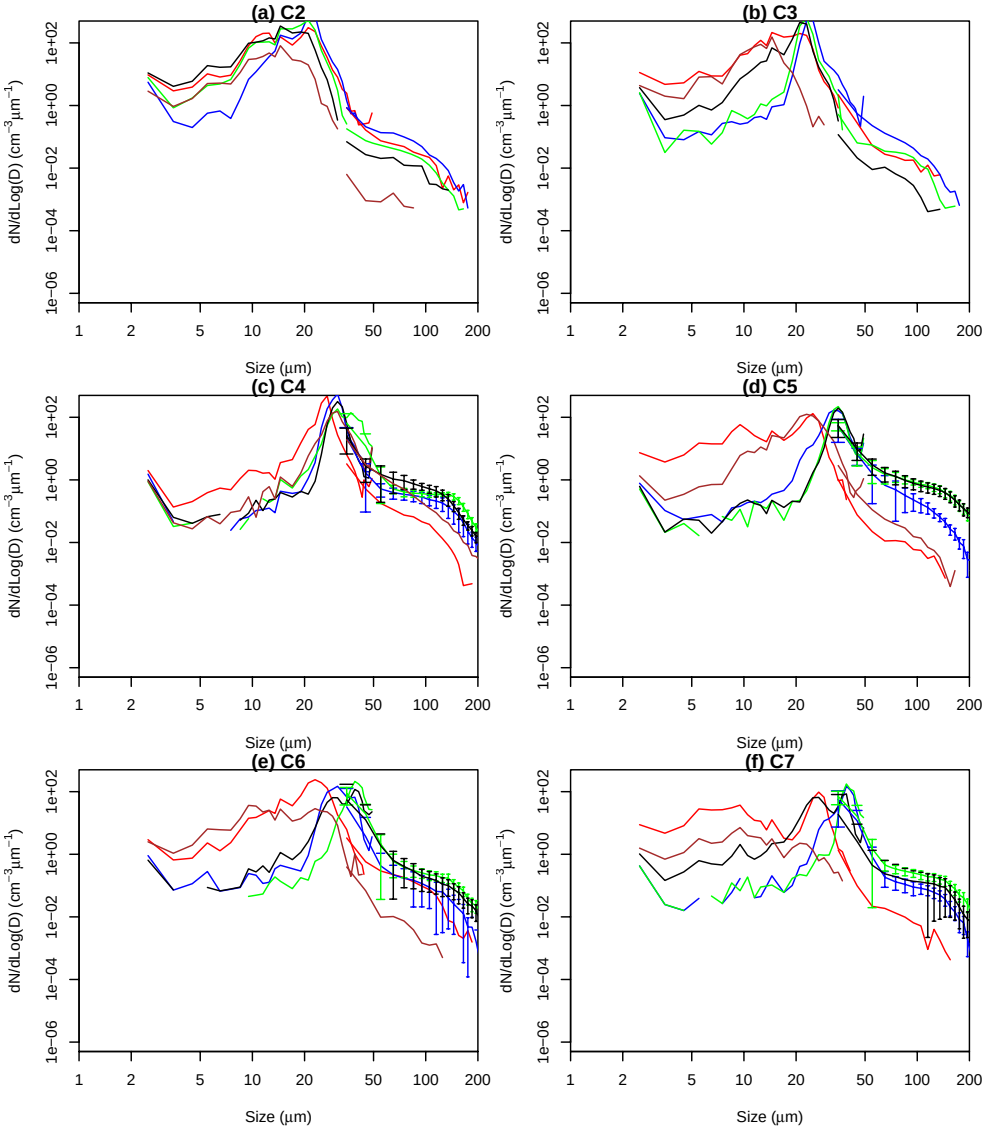

Fig. 6. Integrated size distribution of cloud particles from CDP and 2D-S for clouds 2–7. The traverse of a cloud is divided equally to 8 parts in the horizontal direction. The averaged distributions in five areas are shown for each cloud. These 5 areas are: the first part (the upshear side, in red), the second and the third parts (in blue), the 4th and the 5th parts (the cloud core, in green), the 6th and 7th parts (in black), and the 8th part (the downshear side, in brown). The ranges of standard deviation are added for clouds C4–C7 for particles larger than 50 µm.

(Fig. 4c) and that T and w are not in phase. The peaks in w are generally between the peaks and troughs of T. This structure is the signature of gravity waves, which is consistent with the satellite image (Fig. 1) and existing knowledge of the wave cloud formation mechanism (Holton, 2004). It is noted that measurements of temperature are not accurate within cloud due to wetting effects on the sensor for clouds where $T > 0\,^{\circ}\mathrm{C}$ (e.g. Lenschow and Pennell, 1974; Heymsfield et al., 1979; Lawson and Cooper, 1990; Eastin et al., 2002). In clouds where $T < 0\,^{\circ}\mathrm{C}$, the deiced probe is subject to a further correction when the deicing heat is applied to the housing. The icing effect on the temperature sensor is minimal even though super-cooled water droplets exist at temperatures greater than $-5\,^{\circ}\mathrm{C}$. However, both the CDP and CPI images suggest there were no ice particles present in these wave clouds. Even in clear air, the gravity wave features are see between C2 and C3 in Fig. 4 and before C13 in Fig. 8.

The 2D-S data indicate that the diameters of cloud particles were all less than 180 µm, with the majority of the particles smaller than 30 µm. The concentrations of particles with $50 \leq d \leq 150$ µm were only a few tens per litre. The cloud particle size distributions obtained from the CDP probe during Run 1 are shown in Fig. 5. The highest droplet concentrations were observed in clouds C1–C3 where the drop diameters were generally between 15–25 µm. Larger droplet sizes (between 25–45 µm) were observed in clouds C4–C7 where

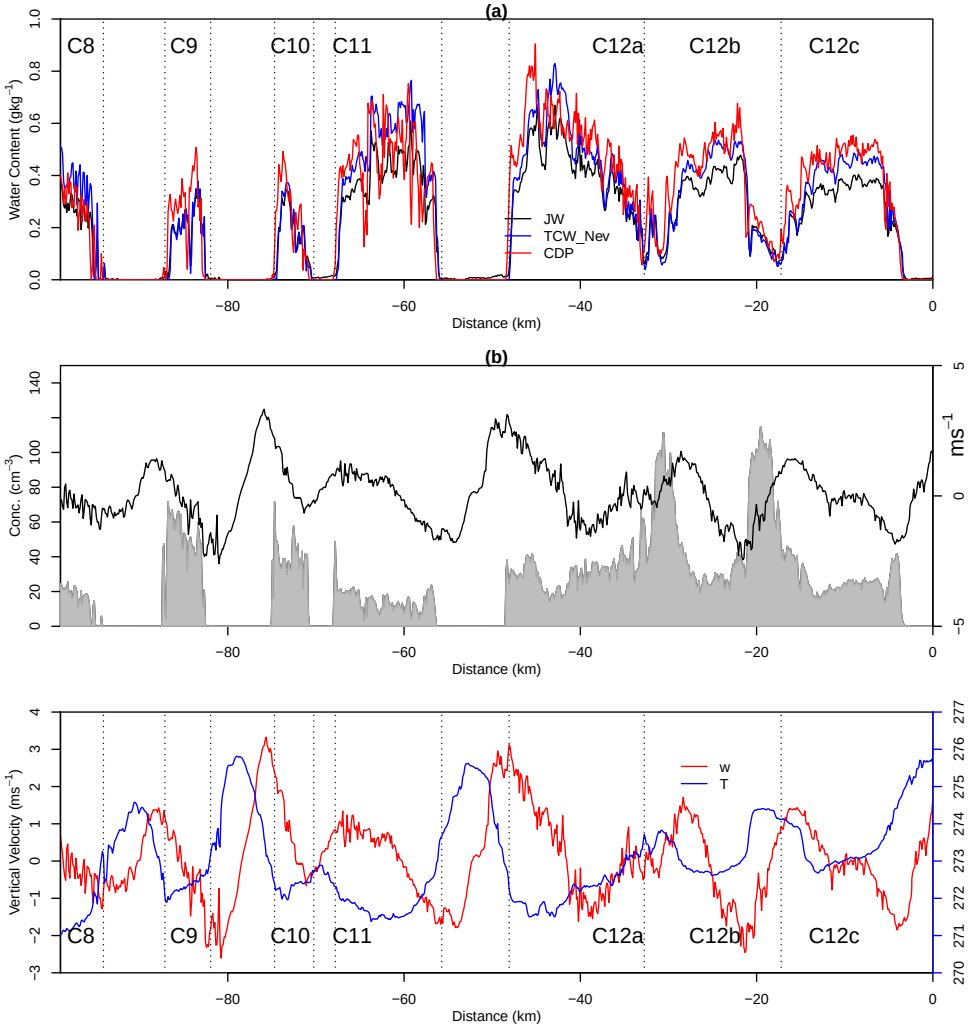

Fig. 7. As in Fig. 4 but for Run 2.

the liquid water contents are higher than in C1–C3. This is illustrated by the calculated mean volume diameters. The size distributions are thus in agreement with the observed LWC and concentrations in Fig. 4, where clouds C1–C3 have lower LWC, compared with clouds C4–C7. To clearly see the size distributions at different locations within the clouds, we have divided up each of the clouds into eight equal parts in the horizontal direction, and then grouped the eight parts into five areas for comparison. These comprise the first and the last areas (first and eighth parts) which are the upshear and downshear regions, respectively. The third area is the core region which occupies the central two (fourth and fifth) parts. The second area covers the two parts (second and third parts) between the upshear and the core regions, and the fourth area (sixth and seventh parts) is between the core and the downshear regions. In each area, the size distributions are averaged to get a mean distribution. The combined size distributions derived from both the CDP and 2D-S data analysed in this way for Run 1 are shown in Fig. 6, which demonstrates favourable agreement in the overlap region of the size distributions. The standard deviations are large for clouds C2 and C3. The overlapping of error bars for drop sizes larger than 50 µm indicates that the differences are not significant in clouds C2 and C3. For clouds C4–C7, drop sizes were larger in the inner parts of the clouds than in the flanks. In cloud C5, the largest drops in size were found in the core and further downwind. Another feature of clouds C4–C7 is that more small droplets were found in the two sides of the clouds. For most clouds, there were more small droplets in the upshear side than in the downshear side.

After a turn and a short profile ascent of 183 m to the next level, the aircraft headed back towards the west for Run 2. A series of penetrations (straight and level runs) were then carried out perpendicular to the two-dimensional crests and troughs of the waves at successively higher altitudes. These were separated by 152 m intervals up to an altitude of about

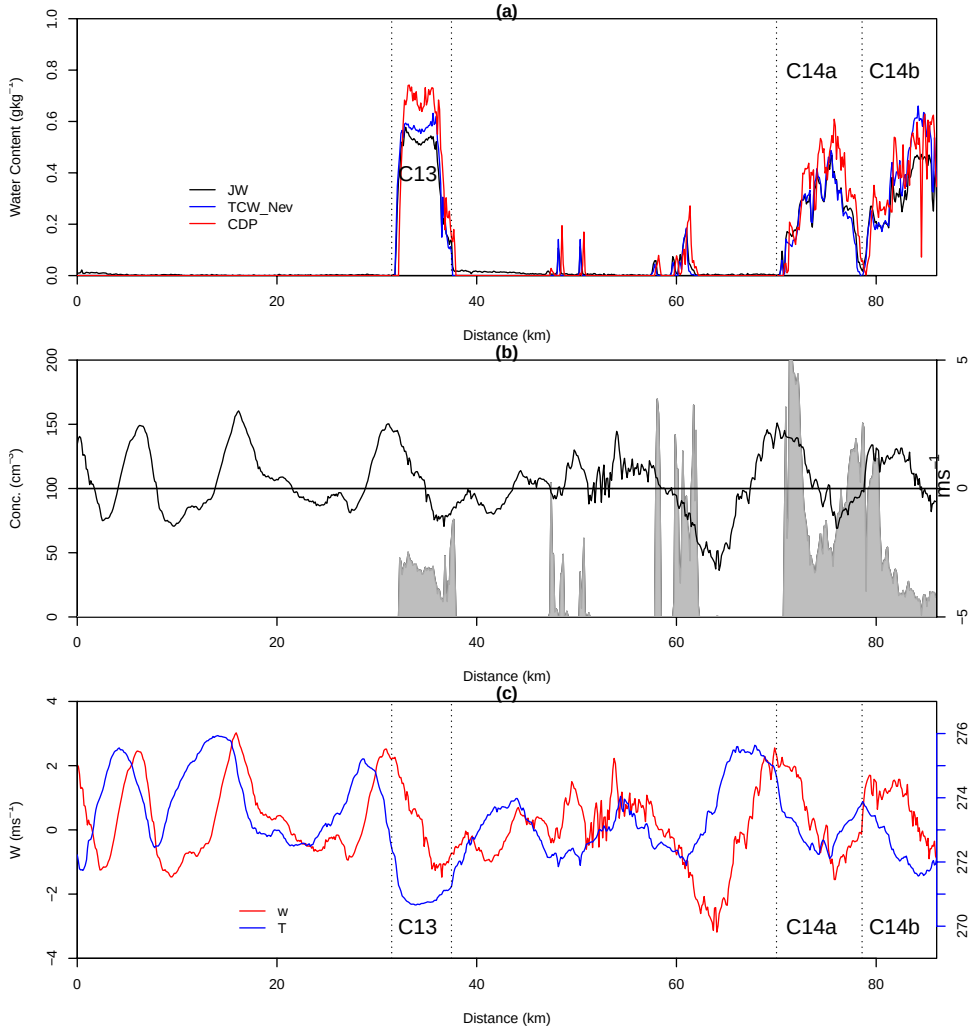

Fig. 8. As in Fig. 4 but for Run 3.

2.6 km a.s.l. In Run 2 (Fig. 7), the vertical velocity with respect to cloud varied in a similar way in clouds C9, C10, and C11 as in clouds C2–C7 in Run 1: the maximum of the updraughts were on the upshear side of the clouds and maximum of the downdraughts were on the downshear side (see Fig. 7), with a gradual change from one to the other. This feature was exhibited in cloud C13 in Run 3 and all clouds in Run 4. Figure 7a and b show that cloud C12 in Run 2 was actually comprised of three separate waves with the same characteristic velocity pattern in each part, but without a clear air/cloud-free region between the downdraught and updraught. Interestingly, the reduction in the liquid water content and also in the concentration of droplets did not coincide with the vertical wind as occured in clouds C9 and C11 in this run, and several clouds in the previous run. It is noted that in cloud C12a there is a dip in the LWC with the dip in vertical velocity. Within the cloud, the vertical velocity shows signs of wave activity (Fig. 7c). It is clear that there were gravity waves within the cloud. The wave activity within clouds was also seen in C14 in Run 3 (Fig. 8). It is not clear what the horizontal extent of the cloud was since the eastern boundary of the cloud was beyond the run. It is also noted that waves existed in the clear air to the west of C13 and between C13 and C14 (Fig. 8). The existence of gravity waves was also seen between C2 and C3 in Run 1 (Fig. 4) and between C15 and C16 in Run 4 (Fig. 9).

The values of LWC are generally higher with the CDP than with the Nevzorov and the Johnson-Williams probes. The discrepancy is very much likely due to the reduced collection efficiency of the Nevzorov and the Johnson-Williams probes and the over-sizing of droplets with the CDP when the equivalent diameters of the drops were dominantly smaller than 45 µm in the clouds.

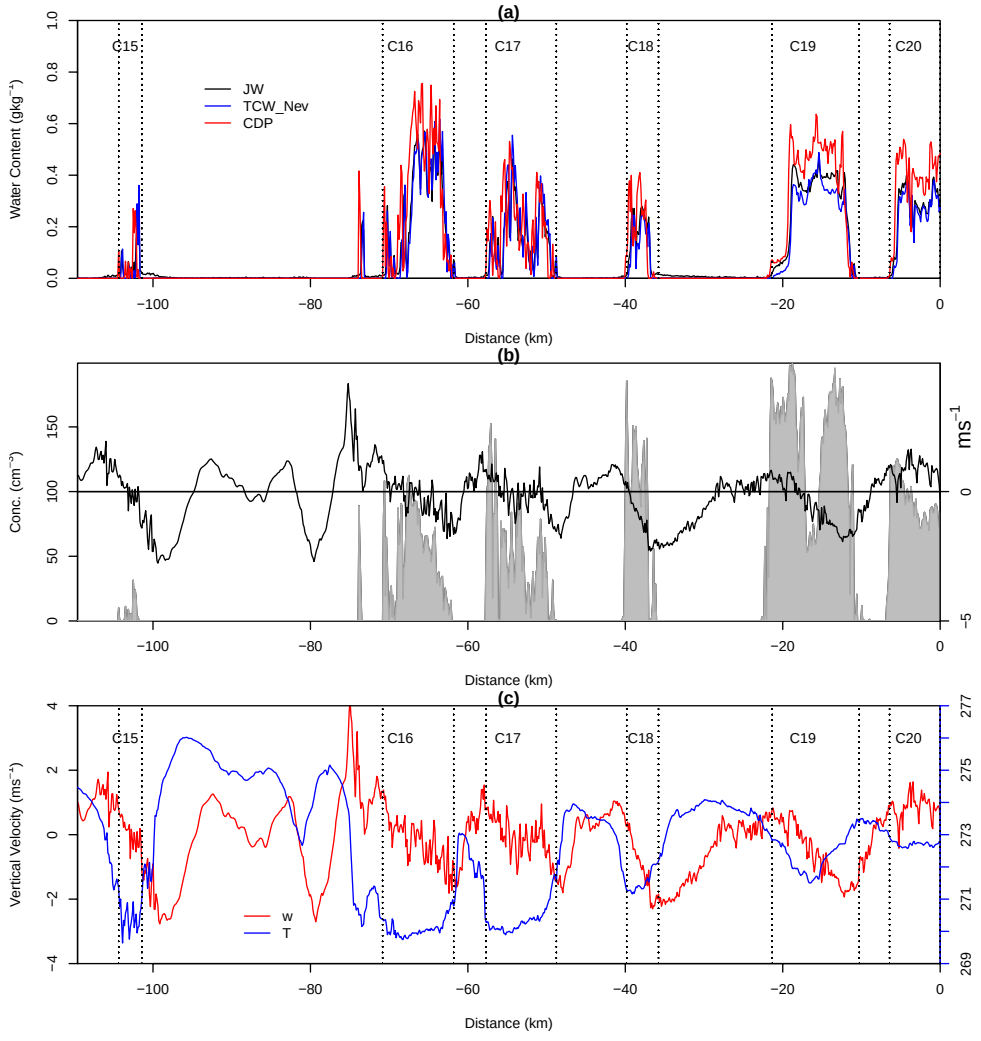

Fig. 9. As in Fig. 5 but for Run 4.

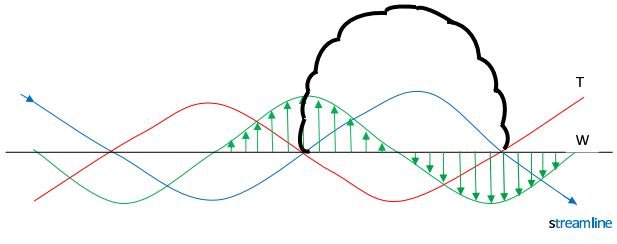

Fig. 10. Ideal structure of a wave cloud. The cloud occurs between the maximum and minimum of vertical velocity, where the temperatures are below the undisturbed mean value.

4 Discussion and conclusion

Observational studies have revealed the importance of gravity waves in cloud dynamics and microphysics (e.g. Heymsfield and Miloshevich, 1993; Gultepe and Starr, 1995; Haag and Kärcher, 2004; Böhme et al., 2004). For a pure gravity wave, the solution (Lin, 2007) can be expressed as

$$w' = w_r \cos(kx + mz - \omega t) - w_i \sin(kx + mz - \omega t) \quad (2)$$

and

$$\theta' = \frac{\theta_0 N^2}{g\omega}[w_r \sin(kx+mz-\omega t) - w_i \cos(kx+mz-\omega t), \quad (3)$$

where w_r and w_i are the real and imaginary parts of $\tilde{w}$, respectively. A typical feature for gravity waves is a phase shift of 90° between temperature and vertical velocity, which has been discussed in details in Lin (2007) and Holton (1992). Figure 10 shows the ideal structure of a wave cloud. There is a phase shift between temperature and vertical velocity. The temperature decreases below the average at the point where the upward motion is strongest, reaches the lowest at the wave crest, and increases to the average where the strongest

downward motion is. A vertical displacement Δz in water-vapour-saturated air will give rise to a change in absolute humidity (Aleksandrova et al., 1992)

$$\mathrm{AH} = \frac{216}{T} e_\mathrm{s} (\Lambda \gamma_\mathrm{a} - \frac{1}{H}) \Delta z, \quad (4)$$

where T is the average temperature, e_s is the saturation vapour pressure, Λ is the temperature-dependence parameter of the saturation vapour pressure, and γ_a is the saturated adiabatic lapse rate. Equation (4) suggests an increase in humidity in the wave crest and a decrease in the wave trough.

The horizontal distribution of vertical velocity across the wave clouds is different from the definition in the Glossary of Meteorology (Glickman, 2000). We found in our study that the maxima in updraughts are on the upshear side and the strong downdraughts are on the downshear side. Apparently, most clouds in our case span approximately between the strongest updraught and strongest downdraught. The results of this paper and the previous studies (Durran and Klemp, 1982; Clark et al., 1986; Heymsfield and Miloshevich, 1995) suggest that a wave cloud forms between the maximum updraught and maximum downdraught in the crest of the wave (Fig. 10).

The gaps between clouds are not uniform in our observations. Gravity waves may play their role in the organization and spacing of the wave clouds. The uneven gaps between clouds are very likely caused by the interaction between cloud and gravity wave as suggested by Clark et al. (1986).

In terms of wave-cloud interaction, we did not measure wind below cloud base because of aircraft operating restrictions. Therefore, it is not possible to confirm the persistent cloud root upward eddies (Clark et al., 1986). However, the horizontal dimension of clouds generally decreases with height. The observations at 4 levels in Runs 1–4 demonstrate the same features in vertical velocity. This indicates that updraughts occur both in front and overhead on the upshear side and downdraughts both in the rear and overhead on the downshear side of the wave clouds.

There are some questions that need further study in the future. For example, what was the relative contribution to the gravity wave generation from topography, from convection, and from other sources? In Runs 2 and 3, waves apparently operated in clouds. It is not known how waves travelled in cloud without significant damping. The interaction between cloud and gravity waves is complex. Clark et al. (1986) noted that "the persistence of the cloud root updraught is quite apparent in spite of the dramatically changing overhead wave field characteristics". In order to better understand the processes, we suggest that measurements (airborne, ground-based or radar) below cloud bases should be carried out in future wave cloud study.

In conclusion, we have analyzed aircraft measurements of wave clouds. We have found that the variations of vertical velocity across wave clouds vary in a distinctive way. The updraughts have maxima on the upshear sides of the clouds and strong downdraughts on the downshear sides. We have also presented the microphysical properties of the clouds. The specific water contents are 0.3–0.8 g kg^{-1}. The concentrations of cloud particles (all drops) are about a couple of hundreds per cubic centimeters. Cloud particles are generally between 15–45 µm in size with only a small proportion reaching drizzle sizes.

Previous studies of wave clouds in mixed- or ice-phase have made progress in understanding the distribution of ice particles and their relationship with ice nuclei. However, it is well known that the parameterization of ice particle formation is difficult because of various freezing modes. Cloud development is much dependent to the freezing schemes (e.g. Cui et al., 2011). Moreover, the discrepancy is large between IN concentration and ice particle concentration, particularly at temperatures greater than $-10\,^\circ$C (Pruppacher and Klett, 1997). The results of ice-free wave clouds presented in this paper provide a case with less complexity and less uncertainty for future numerical simulation of wave cloud and the interaction between wave and cloud. It should be pointed out that a model should be run on a three-dimensional grid since the spectral distribution of kinetic energy in a two-dimensional flow differ fundamentally from a real three-dimensional turbulent flow where the square of vorticities is not obliged to be conserved (Fjortoft, 1953).

Acknowledgements. The work was funded by the Natural Environment Research Council APPRAISE programme, grant number NE/E01125X/1. We would like to thank the DFL pilots and operators of the FAAM BAe146 aircraft and the FAAM staff for assistance in undertaking these measurements with the data and for making the project possible. We thank NCAS and FGAM for their measurements and operators. The UK Meteorological Office provided weather forecast during the field campaign. We are grateful to the British Atmospheric Data Centre for providing access to the APPRAISE-clouds dataset. We would likt to acknowledge the NASA Goddard Earth Science Distributed Active Archive Center for the MODIS Level IB image.

Edited by: T. Garrett

References

Aleksandrova, T. V., Plechkov, V. M., and Stankevich, K. S.: Detection of internal gravity waves in cloud layers according to radiobrightness contrasts of the atmosphere, Radiophys. Quant. Electron., 35, 155–158, doi:10.1007/BF01038019, 1992.

Baker, B. A. and Lawson, R. P.: In Situ Observations of the Microphysical Properties of Wave, Cirrus, and Anvil Clouds. Part I: Wave Clouds, J. Atmos. Sci., 63, 3160–3185, 2006.

Baumgardner, D. and Gandrud, B. E.: A comparison of the microphysical and optical properties of particles in an aircraft contrail and mountain wave cloud, Geophys. Res. Lett., 25, 1129–1132, 1998.

Böhme, T., Hauf, T., and Lehmann, V.: Investigation of short-period gravity waves with the Lindenberg 482 MHz tropospheric wind profiler, Q. J. Roy. Meteorol. Soc., 130, 2933–2952, 2004.

Brown, P. R. A.: Aircraft measurements of mountain waves and their associated momentum flux over the British Isles, Q. J. Roy. Meteor. Soc., 109, 849–865, 1983.

Clark, T. L. and Hauf, T.: Upshear cumulus development: A result of boundary layer/free atmosphere interactions. In: Conf. Radar. Meteorol. Conf. Cloud Phys., 23rd, Snowmass, Colo., J18-J21. Am. Meteorol. Soc., Boston, Massachusetts. Preprints, 1986.

Clark, T. L., Hauf, T., and Kuettner, J. P.: Convectively forced internal gravity waves: Results from two-dimensional experiments, Q. J. Roy. Meteor. Soc., 112, 899–926, 1986.

Connolly, P. J., Flynn, M. J., Ulanowski, Z., Choularton, T. W., Gallagher, M. W., and Bower, K. N.: Calibration of the cloud particle imager probes using calibration beads and ice crystal analogs: The depth of field, J. Atmos. Oceanic Technol., 24, 1860–1879, 2007.

Cooper, W. A. and Saunders, C. P. R.: Winter Storms over the San Juan Mountains. Part II: Microphysical Processes, J. Appl. Meteor., 19, 927–941, 1980.

Cooper, W. A. and Vali, G.: The origin of ice in mountain cap clouds, J. Atmos. Sci., 38, 1244–1259, 1981.

Cotton, W. R., Bryan, G., and van den Heever, S.: Storm and Cloud Dynamics, Academic Press, New York, 820 pp., 2010.

Crawford, I., Bower, K. N., Choularton, T. W., Dearden, C., Crosier, J., Westbrook, C., Capes, G., Coe, H., Connolly, P. J., Dorsey, J. R., Gallagher, M. W., Williams, P., Trembath, J., Cui, Z., and Blyth, A.: Ice formation and development in aged, wintertime cumulus over the UK: observations and modelling, Atmos. Chem. Phys., 12, 4963–4985, doi:10.5194/acp-12-4963-2012, 2012.

Crosier, J., Bower, K. N., Choularton, T. W., Westbrook, C. D., Connolly, P. J., Cui, Z. Q., Crawford, I. P., Capes, G. L., Coe, H., Dorsey, J. R., Williams, P. I., Illingworth, A. J., Gallagher, M. W., and Blyth, A. M.: Observations of ice multiplication in a weakly convective cell embedded in supercooled mid-level stratus, Atmos. Chem. Phys., 11, 257–273, doi:10.5194/acp-11-257-2011, 2011.

Cui, Z., Davies, S., Carslaw, K. S., and Blyth, A. M.: The response of precipitation to aerosol through riming and melting in deep convective clouds, Atmos. Chem. Phys., 11, 3495–3510, doi:10.5194/acp-11-3495-2011, 2011.

Durran, D. R. and Klemp, J. B.: The effects of moisture on trapped mountain lee waves, J. Atmos. Sci., 39, 2490–2506, 1982.

Eastin, M. D., Black, P. G., and Gray, W. M.: Flight-level thermodynamic instrument wetting errors in hurricanes. Part I: Observations, Mon. Weather Rev., 130, 825–841, 2002.

Field, P. R., Cotton, R. J., Noone, K., Glantz, P., Kaye, P. H., Hirst, E., Greenaway, R. S., Jost, C., Gabriel, R., Reiner, T., Andreae, M., Saunders, C. P. R., Archer, A., Choularton, T., Smith, M., Brooks, B., Hoell, C., Bandy, B., Johnson, D., and Heymsfield, A.: Ice nucleation in orographic wave clouds: Measurements made during INTACC, Q. J. Roy. Meteorol. Soc., 127, 1493–1512, 2001.

Field, P. R., Heymsfield, A. J., Shipway, B. J., DeMott, P. J., Pratt, K. A., Rogers, D. C., Stith, J., and Prather, K. A.: Ice in Clouds Experiment-Layer Clouds. Part II: Testing Characteristics of Heterogeneous Ice Formation in Lee Wave Clouds, J. Atmos. Sci., 69, 1066–1079, 2012.

Fjortoft, R.: On the changes in the spectral distribution of kinetic energy for two-dimensional non-divergent flow, Tellus, 5, 225–230, 1953.

Friehe, C. A. and Khelif, D.: Fast-response aircraft temperature sensors, J. Atmos. Oceanic Technol., 9, 784–795, 1992.

Glickman, T. S.: Glossary of Meteorology (Second Edition), American Meteorological Society, Boston, MA, 2000.

Grubišić, V., Doyle, J. D., Kuettner, J., Dirks, R., Cohn, S. A., Pan, L. L., Mobbs, S., Smith, R. B., Whiteman, C. D., Czyzyk, S., Vosper, S., Weissmann, M., Haimov, S., De Wekker, S. F. J., and Chow, F. K.: The Terrain-Induced Rotor Experiment: A Field Campaign Overview Including Observational Highlights, B. Am. Meteor. Soc., 89, 1513–1533, 2008.

Gultepe, I. and Starr, D. O.: Dynamical structure and turbulence in cirrus clouds: Aircraft observations during FIRE, J. Atmos. Sci., 52, 4159–4182, 1995.

Haag, W. and Kärcher, B.: The impact of aerosols and gravity waves on cirrus clouds at midlatitudes, J. Geophys. Res., 109, D12202, doi:10.1029/2004JD004579, 2004.

Heymsfield, A. J. and Miloshevich, L. M.: Relative humidity and temperature influences on cirrus formation and evolution: Observations from wave clouds and FIRE-II, J. Atmos. Sci., 52, 4302–4323, 1995.

Heymsfield, A. J., Dye, J. E., and Biter, C. J.: Overestimates of entrainment from wetting of aircraft temperature sensors in cloud, J. Appl. Meteor., 18, 92–95, 1979.

Heymsfield, A. J., Field, P. R., Bailey, M., Rogers, D. C., Stith, J., Twohy, C., Wang, Z., and Haimov, S.: Ice in Clouds Experiment-Layer Clouds. Part I: Ice growth rates derived from lenticular wave cloud penetrations, J. Atmos. Sci., 68, 2628–2654, 2011.

Holton, J. R.: An Introduction to Dynamic Meteorology, 4th ed, Academic Press, New York, 535 pp., 2004.

Isaac, G. A., Korolev, A., Strapp, J. W., Cober, S. G., Boudala, F. S., Marcotte, D., and Reich, V. L.: Assessing the collection efficiency of natural cloud particles impacting the Nevzorov total water content probe, Proc. 44th AIAA Aerospace Sciences Meeting and Exhibit, Reno, NV, AIAA, 9–12 January 2006, Paper AIAA2006-265, 2006.

Jensen, E. J., Toon, O. B., Tabazadeh, A., Sachse, G. W., Anderson, B. E., Chan, K. R., Twohy, C. W., Gandrud, B., Aulenbach, S. M., Heymsfield, A., Hallett, J., and Gary, B.: Ice nucleation processes in upper tropospheric wave-clouds observed during SUCCESS, Geophys. Res. Lett., 25, 1363–1366, 1998.

Korolev, A. V., Nevzorov, A. N., Strapp, J. W., and Isaac, G. A.: The Nevzorov Airborne Hot-Wire LWC-TWC Probe : Principle of Operation and Performance Characteristics, J. Atmos. Ocean. Techn., 15, 1495–1510, 1998.

Kuettner, J. P., Hildebrand, P. A., and Clark, T. L.: Convection waves : Observations of gravity wave systems over convectively active boundary layers, Q. J. Roy. Meteor. Soc., 113, 445–467, 1987.

Lance, S., Brock, C. A., Rogers, D., and Gordon, J. A.: Water droplet calibration of the Cloud Droplet Probe (CDP) and in-flight performance in liquid, ice and mixed-phase clouds during ARCPAC, Atmos. Meas. Tech., 3, 1683–1706, doi:10.5194/amt-3-1683-2010, 2010.

Lawson, R. P. and Cooper, W. A.: Performance of some airborne thermometers in clouds, J. Atmos. Oceanic Technol., 7, 480–494, 1990.

Lawson P. R., Baker B. A., Schmitt C. G., and Jensen, T. L.: An overview of microphysical properties of Arctic clouds observed in May and July 1998 during FIRE ACE, J. Geophys. Res., 106, 14989–15014, 2001.

Lawson, R. P., O'Connor, D., Zmarzly, P., Weaver, K., Baker, B. A., Mo, Q., and Jonsson, H.: The 2D-S (Stereo) probe: Design and preliminary tests of a new airborne, high-speed, high-resolution imaging probe, J. Atmos. Ocean. Tech., 23, 1462–1477, 2006.

Lenschow, D. H. and Pennell, W. T.: On the measurement of in-cloud and wet-bulb temperatures from an aircraft, Mon. Weather Rev., 102, 447–454, 1974.

Lin, Y. L.: Mesoscale Dynamics, Cambridge University Press, 674 pp., 2007.

Ludlam, F. H.: Clouds and Storms, Pennsylvania State University Press, University Park, PA, 405 pp., 1980.

Politovich, M. K. and Vali, G.: Observations of Liquid Water in Orographic Clouds over Elk Mountain, J. Atmos. Sci., 40, 1300–1312, 1983.

Pruppacher, H. R. and Klett, J. D.: Microphysics of Clouds and Precipitation, 2nd ed, Kluwer Academic, 954 pp., 1997.

Schwarzenboeck, A., Mioche, G., Armetta, A., Herber, A., and Gayet, J.-F.: Response of the Nevzorov hot wire probe in clouds dominated by droplet conditions in the drizzle size range, Atmos. Meas. Tech., 2, 779–788, doi:10.5194/amt-2-779-2009, 2009.

Scorer, R. S.: Theory of waves in the lee of mountains, Q. J. Roy. Meteorol. Soc. 75, 41–56, 1949.

Shutts, G. and Broad, A.: A case study of lee waves over the Lake District in northern England, Q. J. Roy. Meteorol. Soc., 119, 377–408, 1993.

Strapp, J. W. and Schemenauer, R. S.: Calibrations of Johnson-Williams liquid water content meters in a high-speed icing tunnel, J. Appl. Meteor, 21, 98–108, 1982.

Stromberg, I. M., Mill, C. S., Choularton, T. W., and Gallagher, M. W.: A case study of stably stratified airflow over the Pennines using an instrumented glider, Boundary-Lay. Meteorol., 46, 153–168, 1989.

Twohy, C. H., Schanot, A. J., and Cooper, W. A.: Measurement of Condensed Water Content in Liquid and Ice Clouds Using an Airborne Counterflow Virtual Impactor, J. Atmos. Oceanic Technol., 14, 197–202, 1997.

Vosper, S. B. and Parker, D. J.: Some perspectives on wave clouds, Weather, 57, 3–8, 2002.

Weston, K. J.: An Observational Study of Convective Cloud Streets, Tellus, 32, 433–438, 1980.

Westbrook, C. D. and Illingworth, A. J.: Evidence that ice forms primarily in supercooled liquid clouds at temperatures $> -27°$C, Geophys. Res. Lett., 38, L14808, doi:10.1029/2011GL048021, 2011.

Wood, N.: Wind flow over complex terrain: A historical perspective and the prospect for large-eddy modelling, Bound.-Lay. Meteor., 96, 11–32, 2000.

Worthington, R.: Alignment of mountain wave patterns above Wales: A VHF radar study during 1990–1998, J. Geophys. Res., 104, 9199–9212, 1999.